Journal of Sound and Vibration (2001) **243**(3), 441–459
doi:10.1006/jsvi.2000.3429, available online at http://www.idealibrary.com on IDEAL®

ACOUSTIC IMPEDANCE MEASUREMENT, PART II: A NEW CALIBRATION METHOD

J.-P. DALMONT

Institut d'Acoustique et de Mécanique, Laboratoire d'Acoustique de l'Université du Maine (UMR CNRS 6613), Avenue Olivier Messiaen, F-72085 Le Mans Cedex 9, France.
E-mail: jean-pierre.dalmont@univ-lemans.fr

(*Received* 9 *March* 2000, *and in final form* 4 *October* 2000)

A calibration method for input impedance sensors which permits an accurate determination of the calibration parameters is presented. The method is based on the measurement of two closed tubes of different lengths whose propagation constant is not required to be accurately known. This method is shown to be applicable to most of the impedance sensors in the literature and is extended to transfer impedance calibration which is needed for multi-post characterization. The method is applied to an impedance sensor using a half-inch microphone cartridge as a source of volume velocity. The attenuation constant of a straight tube is measured and shown to be less than 3% larger than results derived from theory of viscothermal dissipation. As an example of two-port characterization, the calibrated sensor, complete with a microphone for transfer impedance measurement, is used for the measurement of side hole parameters.

1. INTRODUCTION

Calibration of impedance measurement set-ups has been the subject of very few papers but has been discussed briefly in some papers [1–7]. Yet this is a crucial step to reach a high level of accuracy. Different methods can be found in the literature which are often limited to a partial determination of the calibration parameters. For analogue devices, mostly only the first order response (see reference [8] for definition) is determined (see for example references [6, 9]). For multi-microphone techniques mostly only the relative response of the microphones is calibrated [10–14] and sometimes the wave constant in the tube between the microphones is determined. On the other hand, Gibiat and Laloë [3] propose a complete calibration method for impedance sensors with three known loads which leads to a large number of calibration parameters (three complex parameters for each frequency).

In the present paper, a calibration method is proposed which was firstly designed to complete and improve the calibration of impedance sensors with volume velocity sources [5]. The aim of the proposed calibration procedure is to obtain an accurate calibration with a reduced number of calibration parameters. The proposed method is an improvement of the one-tube method described in Part I. From a rough calibration using this method a first evaluation of the reduced input impedance of a long tube is obtained which seems to be little different from the theory. This calibration may be considered to be sufficient but calculating the hyperbolic arctangent function of both experimental and theoretical impedance emphasizes the difference between the two curves (Figures 1 and 2). The result issued from experiment can be used as an error function. It is shown, in section 2, how well chosen

0022-460X/01/230441 + 19 $35.00/0

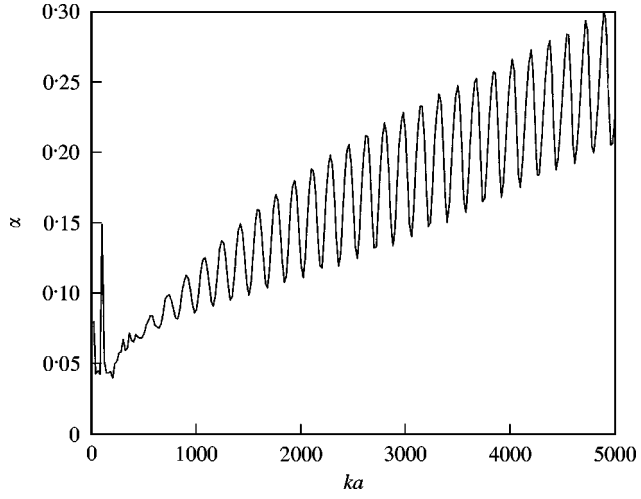

Figure 1. Experimental value of $\alpha = \mathrm{Re}[\mathrm{arctanh}(Z_e/Z_c)]/\ell$ for a closed 1 m tube of radius 0·01 m versus reduced frequency ka after an incomplete and inaccurate calibration.

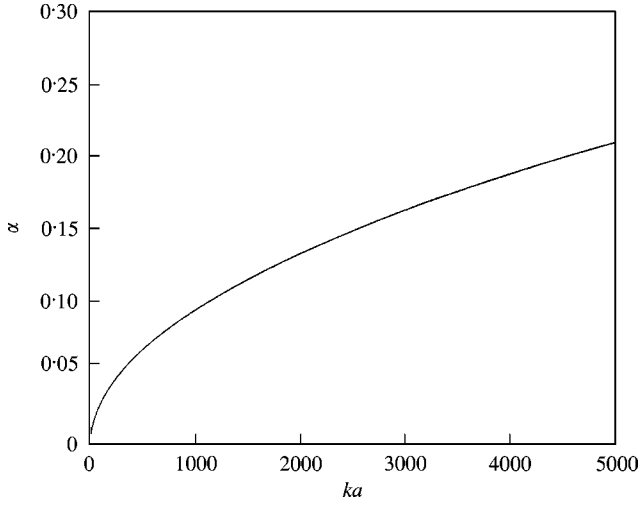

Figure 2. Theoretical value of the attenuation constant α of a closed tube of radius 0·01 m versus reduced frequency ka.

calibration parameters can be related to this error function and, in section 3, how these parameters can be determined. A second, short, tube is measured to limit the errors due to the temperature measurement. This allows the determination of the propagation constant of the tube. To allow multi-port characterization, the calibration procedure is extended to transfer impedance measurements (section 4). In section 5, the calibration is applied to a sensor using a capacitive microphone cartridge as a source for input and transfer impedance measurements [15]. An application to the determination of the series and shunt inductances of the equivalent circuit of a side hole is presented (section 6).

2. THEORY

As discussed in Part I, an impedance set-up can be defined as a system with two entries whose signals e and u are linearly related to pressure P and volume velocity U at the input

of the measured system:

$$\begin{pmatrix} e \\ u \end{pmatrix} = \begin{pmatrix} m & n \\ p & q \end{pmatrix} \begin{pmatrix} P \\ U \end{pmatrix}. \tag{1}$$

The matrix $\left(\begin{smallmatrix} m & n \\ p & q \end{smallmatrix}\right)$ which relates the two signals to the measured quantities is the "response" matrix.

In this section it is first shown, as an example, how calibration errors influence the measured impedance of a calibration tube. By analogy with this example, an expression for the "response matrix" of the sensor involving four parameters whose effects can be separated is given (equation (10)). Finally, an expression for the arctangent of the measured impedance as a function of the calibration parameters, on which the calibration method is based, is derived (equation (14)).

2.1. CASE OF TWO IDEAL SENSORS ON A STRAIGHT TUBE

Consider a sensor made with two ideal transducers: one for pressure and one for volume velocity. If both are located at the reference plane, the representative matrix of the sensor is given by

$$\begin{pmatrix} m & n \\ p & q \end{pmatrix} = \begin{pmatrix} R_e & 0 \\ 0 & R_u \end{pmatrix}, \tag{2}$$

where R_e and R_u are the response of the pressure transducer and the volume velocity transducer respectively.

With such an ideal sensor the measured impedance Z_{mes} is given by

$$Z_{mes} = \frac{R_e e}{R_u u} = \frac{P}{U} = Z. \tag{3}$$

If the calibration of the transducers is not perfect there is a slight difference between the estimated value of R_e and R_u and their exact value. This leads to

$$Z_{mes} = XZ, \tag{4}$$

where X is a complex number (possibly frequency dependent) which is, if the calibration is not too poor, close to unity. This, applied to a tube of length L closed with an infinite impedance (see Appendix B), leads to

$$Z_{mes} = XZ = XZ_c \coth(\Gamma L). \tag{5}$$

Assuming X to be a real number larger than unity, the maxima of Z_{mes} are larger than the maxima of Z ("resonances") which could be interpreted as the consequence of a lower damping ($(\alpha L)_{mes} \cong Z_c/Z_{mes} = Z_c/(XZ) \cong \alpha L/X$). Also, the minima of Z_{mes} are larger than the minima of Z ("antiresonances") which could be interpreted as the consequence of larger damping ($(\alpha L)_{mes} \cong Z_{mes}/Z_c = XZ/Z_c = X\alpha L$). When plotting $(\alpha L)_{mes} = \mathrm{Re}(\mathrm{arctanh}(Z_{mes}/Z_c))$ versus frequency the curve appears to oscillate between $\alpha L/X$ (resonances) and $X\alpha L$ (antiresonances). In the same way, if X is complex the argument of X will imply oscillations on $(kL)_{mes} = \mathrm{Im}(\mathrm{arctanh}(Z_c/Z_{mes}))$.

Consider now that both transducers are on a straight tube whose characteristic impedance and propagation constant are Z_c and Γ, respectively, but not exactly on the same

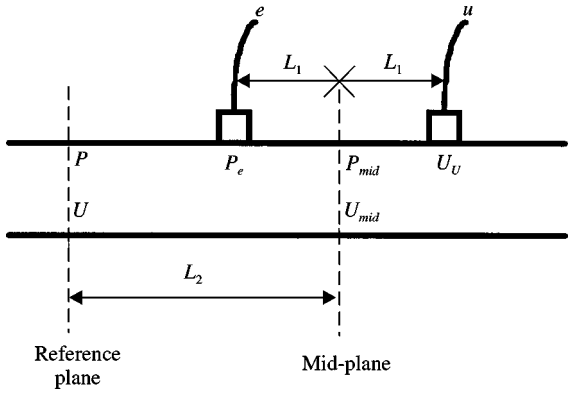

Figure 3. Schematic drawings and notations for an impedance sensor with pressure and volume velocity transducers at different abscissae.

plane. Pressure P_{mid} and volume velocity U_{mid} at an equal distance L_1 from both transducers are related to pressure P_e and volume velocity U_u on the transducers by the following equations (see Figure 3):

$$\begin{aligned} P_e &= \cosh(\Gamma L_1) P_{mid} + Z_c \sinh(\Gamma L_1) U_{mid}, \\ U_u &= -\sinh(\Gamma L_1) P_{mid}/Z_c + \cosh(\Gamma L_1) U_{mid}. \end{aligned} \tag{6}$$

Setting the origin at equal distance from both transducers leads to the following response matrix of the transducer:

$$\begin{pmatrix} m & n \\ p & q \end{pmatrix} = \begin{pmatrix} R_e & 0 \\ 0 & R_u \end{pmatrix} \begin{pmatrix} \cosh \Gamma L_1 & Z_c \sinh \Gamma L_1 \\ \dfrac{-1}{Z_c} \sinh \Gamma L_1 & \cosh \Gamma L_1 \end{pmatrix}. \tag{7}$$

Measured impedance $Z_{mes} = P_e/U_u = R_e e/R_u u$ of a closed tube of length L is then given by

$$Z_{mes} = \frac{\cosh[\Gamma(L + L_1)]}{\sinh[\Gamma(L - L_1)]}. \tag{8}$$

Measured resonance frequencies (frequencies for which $|Z_{mes}|$ is maximum) correspond to a length $L - L_1$ and, similarly, measured antiresonance frequencies (frequencies for which $|Z_{mes}|$ is minimum) correspond to a length $L + L_1$. Consequently, when plotting $(kL)_{mes} = \mathrm{Im}(\mathrm{arctanh}(Z_c/Z_{mes}))$ versus frequency the curve appears to oscillate between $k(L - L_1)$ (resonances) and $k(L + L_1)$ (antiresonances).

Finally, if the reference plane is considered to be at a distance L_2 from the mid point between the two transducers (see Figure 3), the response matrix is given by

$$\begin{pmatrix} m & n \\ p & q \end{pmatrix} = \begin{pmatrix} R_e & 0 \\ 0 & R_u \end{pmatrix} \begin{pmatrix} \cosh \Gamma L_1 & Z_c \sinh \Gamma L_1 \\ \dfrac{-1}{Z_c} \sinh \Gamma L_1 & \cosh \Gamma L_1 \end{pmatrix} \begin{pmatrix} \cosh \Gamma L_2 & Z_c \sinh \Gamma L_2 \\ \dfrac{1}{Z_c} \sinh \Gamma L_2 & \cosh \Gamma L_2 \end{pmatrix}. \tag{9}$$

It is easy to understand that changing the reference plane does not induce oscillations because it simply adds kL_2 to $\mathrm{Im}(\mathrm{arctanh}(Z_c/Z))$.

2.2. RELATION BETWEEN THE AMPLITUDE OF THE OSCILLATIONS AND THE CALIBRATION PARAMETERS

Equation (9) is interesting because it separates errors on the location of the transducers from transducer responses. It can be generalized to every transducer, L_1 and L_2 being considered as complex and frequency-dependent quantities. Finally, the representative matrix can be arbitrarily written (although this is justified *a posteriori*) as follows:

$$\begin{pmatrix} m & n \\ p & q \end{pmatrix} = \begin{pmatrix} R_e & 0 \\ 0 & R_u \end{pmatrix} \frac{1}{\sqrt{\cosh 2d}} \begin{pmatrix} \cosh d & Z_c \sinh d \\ \dfrac{-1}{Z_c} \sinh d & \cosh d \end{pmatrix} \begin{pmatrix} \cosh b & Z_c \sinh b \\ \dfrac{1}{Z_c} \sinh b & \cosh b \end{pmatrix}. \quad (10)$$

The term $1/\sqrt{\cos 2d}$ has been introduced to compensate for the determinant of the second matrix of the right term which is not equal to unity. The response matrix and its inverse matrix have then a similar form.

The aim is now to obtain the calibration parameters R_e, R_u, b and d. For a straight closed tube of length L terminated by the admittance Y_t, the input impedance is given by: $Z = Z_c \coth(\Gamma L + \operatorname{arctanh}(Z_c Y_t))$ where Y_t is the termination admittance (see Appendix B). Setting $H = e/u$ and $z_r = Z/Z_c$ and using equation (10), it can be rewritten as

$$H = Z_c K e^g \frac{z_r' + \tanh d}{1 - z_r' \tanh d} \quad (11)$$

with

$$K e^g = \frac{R_e}{R_u} \quad \text{and} \quad z_r' = \frac{z_r + \tanh b}{1 + z_r \tanh b}.$$

For the calibration tube, z_r' is given by

$$z_r' = \coth(\Gamma L') \quad \text{with} \quad \Gamma L' = \Gamma L + \operatorname{arctanh}(Z_c Y_t) + b. \quad (12)$$

KZ_c is obtained from a first determination of R so that g is not too large. In practice, it is sufficient that the magnitude of K is such that the minima of H/KZ_c expressed in dB are negative and the maxima are positive and in the same manner the minima of the argument of H/KZ_c are negative and the maxima are positive. The parameter b is complex and frequency dependent. As the real part of b/Γ can be interpreted as a length correction, the choice of the origin of the longitudinal co-ordinate influences the value of this term.

It can be demonstrated (see Appendix C) that H can be approximated, if $g \ll 1$ and $d \ll 1$, by

$$H \cong KZ_c \coth[\Gamma L' - d \cosh(2\Gamma L') - 1/2g \sinh(2\Gamma L')], \quad (13)$$

where

$$\Gamma L' = \Gamma L + \operatorname{arctanh}(Z_c Y_t) + b.$$

Writing $\Gamma L' = \mathrm{j}kL' + \alpha L'$ and assuming that $\alpha L' \ll 1$ (this approximation is not necessary but is used here for clarity; exact equations (C1a) and (C1b) are given in Appendix C) it can

be written that

$$\mathrm{Re}\left(\operatorname{arctanh}\left(\frac{H}{KZ_c}\right)\right) \cong \alpha L' - \mathrm{Re}(d)\cos(2kL') + \frac{1}{2}\mathrm{Im}(g)\sin(2kL') \tag{14a}$$

and

$$\mathrm{Im}\left(\operatorname{arctanh}\left(\frac{H}{KZ_c}\right)\right) \cong kL' - \mathrm{Im}(d)\cos(2kL') - \frac{1}{2}\mathrm{Re}(g)\sin(2kL'). \tag{14b}$$

Periodic oscillations appear in plotting the real and imaginary parts of $\operatorname{arctanh}(H/KZ_c)$ against frequency (see Figure 1 for the real part). The amplitude of these oscillations is proportional to d and g and their period, in the frequency domain, is related to the frequency and to the equivalent length of the tube L'.

3. DESCRIPTION OF THE METHOD

After a first approximate calibration and the measurement of a long closed tube the quantity H/KZ_c (crude measured impedance) is obtained. Then real and imaginary parts of the hyperbolic arctangent are calculated (equations (14a) and (14b) in which oscillations can be detected. The complex amplitude of these oscillations can be determined using a synchronous demodulation. This consists of multiplying these quantities by estimates of $\sin(2kL')$ and $\cos(2kL')$ and then using a low-pass filter. The real part of d and the imaginary part of g are then obtained from equation (14a). The imaginary part of d and the real part of g are obtained from equation (14b). If $\alpha L'$ is not small this is more complex but it can be solved. The low-pass filter will be efficient if at least one period of the oscillations is considered (this is sufficient because an iterative process is used). So the number of calibration points is proportional to the length L of the tube. This is especially important for low-frequency calibration because the first calibration point will correspond approximately to the first resonance frequency of the tube $f = c/2L$. For example, with a 2 m tube the first calibration point is obtained for approximately 80 Hz. The estimate of kL' can be obtained from a low-pass filtering of the imaginary part of the hyperbolic arctangent of H/KZ_c. As equation (13) is an approximation assuming d to be small compared to unity and as synchronous detection, because of the windowing associated to the low-pass filter, does not give the exact amplitudes, parameters obtained are not exact. An iterative process is then needed: from the first evaluation of d and g, a new evaluation of the reduced impedance z'_r (H/KZ_c being the first evaluation) is deduced, from which corrective terms Δd and Δg are deduced which, added to the previous evaluation of d and g, give their new evaluation and so on. The process is stopped when Δd and Δg are small enough. In practice, 10 steps are enough. At the end of the process an estimation of parameters d and g is obtained.

The parameter b remains to be determined. It could be deduced theoretically from the theoretical evaluation of the wave constant Γ_{theo} and of the hyperbolic arctangent of the reduced termination admittance Z_cY_t: $b = \operatorname{arctanh}(z_r) - \Gamma_{theo}L - \operatorname{arctanh}(Z_cY_t)$. For a rigid wall, Z_cY_t can be ignored to a good approximation. This method may not be accurate enough in practice because the theoretical determination of the wave constant depends on the temperature. So an error in the temperature evaluation implies an error in b proportional to the tube length. For example, using a tube of length $L = 1$ m, a 1°C error in temperature implies an error of 1·7 mm on the equivalent length correction $\mathrm{Re}(b/\Gamma)$; that is an error of 1·7 mm on the reference abscissa of the measurement. For some measurements this error may be too large. Another solution is to measure a short tube of length ℓ and the

same diameter. The parameter b is then deduced by writing

$$b + \operatorname{arctanh}(Z_c Y_t) = \frac{L \operatorname{arctanh}(z_r'(\ell)) - \ell \operatorname{arctanh}(z_r'(L))}{L - \ell}, \tag{15}$$

where $z_r'(L) = \coth[\Gamma L + \operatorname{arctanh}(Z_c Y_t) + b]$ and $z_r'(\ell) = \coth[\Gamma \ell + \operatorname{arctanh}(Z_c Y_t) + b]$ are the experimental evaluations of z_r' for tubes of lengths L and ℓ respectively.

It is not necessary to measure the absolute value of the temperature, but its stability must be checked during the measurements. Nevertheless, the accuracy is better than with the first method even if some undetected temperature fluctuations occur during measurements. For example, a 1°C change in temperature between the two measurements implies an error in the equivalent length correction $\mathrm{Re}(b/\Gamma)$ of 0·15 mm for $L = 1$ m and $\ell = 0{\cdot}085$ m.

It must be pointed out that the determination of parameter b implies that the termination admittance is known. As this admittance is small for a closed tube it can be replaced by its theoretical evaluation for a rigid wall, namely $Z_c Y_t = 9{\cdot}6 \times 10^{-6} \sqrt{f}(1 + j)$ at 20°C, with good accuracy (f is the frequency in Hz; see for example reference [16] p. 242 with numerical values from reference [9]). The imaginary part corresponds to an equivalent length of 0·05 mm for a 10 mm radius tube at 100 Hz and the real part is equivalent to the dissipation on a length of 3 mm for a tube of 10 mm radius. Thus, it can be understood that assuming $Z_c Y_t = 0$ is sufficient for most applications.

This method also permits the determination of the propagation constant which is given by

$$\Gamma = \frac{\operatorname{arctanh}(z_r'(L)) - \operatorname{arctanh}(z_r'(\ell))}{L - \ell}. \tag{16}$$

As an application the measurement of the wave constant of a cylindrical tube is given in section 5.2.

To achieve the calibration, the function K is deduced from KZ_c if Z_c is known. The assumption here is that if the difference between the theoretical and the experimental wave constant Γ is small then the difference between the theoretical and the experimental characteristic impedance Z_c is also small. Thus, the theoretical expression of Z_c can be used. This assumption seems reasonable because both Γ and Z_c are related to the same quantities: $\Gamma = \sqrt{Z_v Y_h}$ and $Z_c = \sqrt{Z_v / Y_h}$ where Z_v and Y_h are, respectively, the series impedance and the shunt admittance per unit length (see for example reference [9]).

Since the calibration procedure gives at most only one calibration point for each resonance frequency of the tube, the question is how to deduce a calibration function from the discrete determination of the calibration parameters. A linear interpolation between two successive calibration points can be done but it is more effective to fit the points with a polynomial function or with a function deduced from a theoretical modelling of the calibrated sensor. This last solution is probably the best way. In the present work, because a complete theoretical model is not available, a polynomial fit of the parameters is chosen. It is done at every step of the iteration process because it has been found that results are better than when the fitting is done at the end of the process. It is clear that the polynomial fitting will be efficient only if calibration functions vary slowly with frequency. This limitation does not exist if fit functions are deduced from a theoretical modelling of the sensor. However, if the fit functions are not efficient, remaining oscillations will appear on the real and imaginary parts of the hyperbolic arctangent of H/KZ_c.

The main advantage of the method is that it is not necessary to know exactly the wave constant and the temperature. Specifically the speed of sound, which is very dependent on

the temperature, and the attenuation constant, which may depend on the wall characteristics, need not be known. A limitation is that the calibration cannot be achieved below the first resonance frequency of the main calibration tube. For a low-frequency calibration very long tubes are needed which is inconvenient. The calibration procedure is not absolutely general because parameters β and δ should not be too large. However, it can be used for most of the known volume velocity source set-ups and also for the two-microphone method (see Part I) and probably for many other techniques.

4. CALIBRATION PROCEDURE FOR TRANSFER IMPEDANCE MEASUREMENTS

The measurement of a N-port is classically done with N impedance sensors fixed on each port of the element to be measured. For a N-port $N(N-1)$ transfer functions are needed. Besides calibration of each impedance sensor the relative response R_{e_i}/R_{u_j} of pair of transducers of two different ports i, j is also needed. A method is now presented based on the measurement of the transfer impedance of a tube which allows the calibration of this relative response. Considering two given ports 1 and 2, the four signals e_1, u_1, e_2, u_2 of the two impedance sensors are linearly related to the transfer matrix by the relation:

$$\begin{pmatrix} e_1 \\ u_1 \end{pmatrix} = \begin{pmatrix} m_1 & n_1 \\ o_1 & p_1 \end{pmatrix} \begin{pmatrix} A & -B \\ C & -D \end{pmatrix} \begin{pmatrix} m_2 & n_2 \\ o_2 & p_2 \end{pmatrix}^{-1} \begin{pmatrix} e_2 \\ u_2 \end{pmatrix}, \tag{17}$$

where

$$\begin{pmatrix} m_1 & n_1 \\ o_1 & p_1 \end{pmatrix} \quad \text{and} \quad \begin{pmatrix} m_2 & n_2 \\ o_2 & p_2 \end{pmatrix}$$

are the calibration matrices of the two sensors and

$$\begin{pmatrix} A & -B \\ C & -D \end{pmatrix}$$

is the transfer matrix of the measured element using a symmetrical orientation for the ports (see Appendix A).

To determine the calibration parameters a straight tube of length L is placed between the two sensors.

Using equation (10) for both ports 1 and 2, it can be derived, after setting $u_2 = 0$, that

$$\cosh(\Gamma L + b_1 + b_2 + d_2)\frac{e_2}{u_1} = \frac{R_{e_2}}{R_{u_1}} Z_c \frac{z'_{1r}}{1 - z'_{1r}\tanh d_1} \frac{\sqrt{\cosh 2d_1 \cosh 2d_2}}{\cosh d_1} \tag{18}$$

with $z'_{1r} = \coth(\Gamma L + b_1 + b_2 + d_2)$, the transfer matrix being given by

$$\begin{pmatrix} A & -B \\ C & -D \end{pmatrix} = \begin{pmatrix} \cosh \Gamma L & -Z_c \sinh \Gamma L \\ \sinh \Gamma L / Z_c & -\cosh \Gamma L \end{pmatrix}. \tag{19}$$

The left-hand side of equation (18) is similar to equation (10) except that the term $\tanh d_1$ is not present in the numerator. However, a procedure similar to the previous one can be applied to $(e_2/u_1 \cosh(\Gamma L + b_1 + b_2 + d_2)$ with only two calibration functions instead of three. Thus, only a long tube measurement is needed. This procedure uses the previous determination of the quantity $\Gamma L + b_1 + b_2 + d_2$ which is deduced from the calibration of

the impedance set-ups of ports 1 and 2. The response $R_{e_2}/R_{u_1}\sqrt{\cosh 2d_1 \cosh 2d_2}/\cosh d_1$ is then obtained, and R_{e_2}/R_{u_1} can be deduced knowing d_1 and d_2. Parameter d_1 can be checked with the first determination.

For symmetrical and reciprocal two-ports measurements the calibration procedure can be simplified: Z_{11} and Z_{12} are sufficient to characterize the two ports. In that case there is no need to have two impedance sensors. Only a second microphone is necessary instead of the second impedance sensor. In that case and if the microphone is small enough it can be assumed that d_2 and b_2 are equal to zero. This amounts to assuming the impedance of the microphone to be infinite. This can be checked by comparing the input impedance of the tube closed by a rigid cap and the input impedance of the tube closed by a rigid cap with the microphone in it.

5. CALIBRATION OF A SENSOR

Calibration results are now shown for an input impedance sensor, complemented for symmetrical two port measurements, with a microphone placed at the closed end of the element to be measured.

5.1. DESCRIPTION OF THE APPARATUS

The sensor used is the one described by Dalmont and Bruneau [15]. It uses a half-inch electrostatic microphone cartridge (condenser microphone) as a source of volume velocity and two small electret microphones as pressure sensors, only one of which may be used, as in the following experiments, or both simultaneously. The source microphone cartridge and the two electret microphones are fixed in a metal plane which constitutes the reference plane for the measurements. Microphone and source are placed as close as possible to the reference plane but some small extra volumes remain between microphones membranes and this plane. The use of a microphone cartridge is attractive because its frequency response is rather flat for frequencies above 100 Hz which simplifies the calibration and also because its mechanical impedance is relatively high. The limitation of this kind of source is that, assuming a constant input voltage, the volume velocity is proportional to the frequency and then at lower frequencies tends to zero with frequency. Measurements for low frequencies, typically lower than 100 Hz, remain difficult for large tubes except around resonance frequencies.

For both excitation and demodulation a dual-phase lock-in amplifier with a sine source is used. An amplifier (BK 2713) whose frequency response is flat for frequencies above 100 Hz and allowing capacitive loads is placed between sine output and source. The two measured signals for input impedance measurements are, respectively, the microphone signal e_1 (after a preamplification) measured with the lock-in amplifier and the amplitude of the reference signal u_1 which is for convenience taken constant. A consequence is that the impedance sensor includes the amplifier. As the amplifier has a flat response for high frequency this will not be a problem. However, the low cut-off frequency has to be determined and corrected before using the calibration procedure. This was done because the calibration procedure is not very efficient for low frequencies. In that case the amplifier was calibrated.

Calibration measurements consist of the measurement of a long brass tube of 1 or 2 m long and a short tube of 0·085 m long both of 20 mm I.D. and 1 mm wall thickness (standard tubing from a hardware shop). They are terminated with a thick PVC cap which is assumed

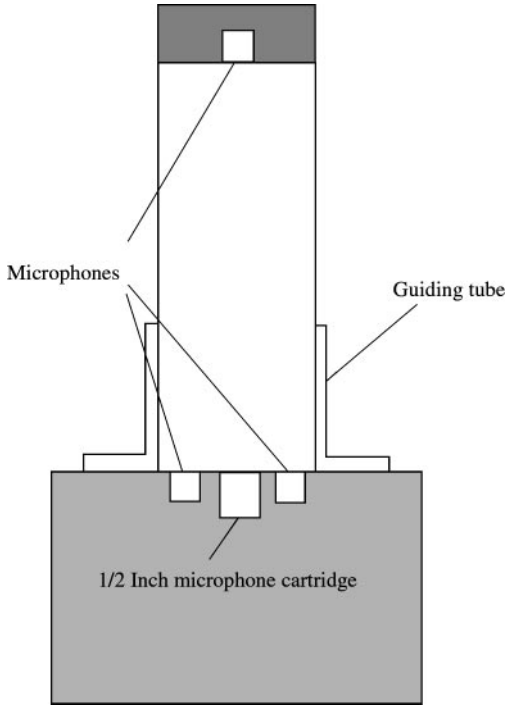

Figure 4. Schematic drawing of the set-up for symmetrical two-port measurement.

to be perfectly rigid. Calibration is valid only for this diameter input because higher modes amplitudes depend on the diameter (see Part I and reference [15]. Both tubes are fixed on the measurement set-up with the same guiding tube of length 30 mm and I.D. 22 mm, which is not removed between measurements (see Figure 4). When transfer measurements have to be made the cap is replaced with another cap with a hole in the centre in which a microphone is fixed. Measurements are made in an anechoic chamber. Temperature is frequently checked. The tubes are placed in the anechoic room at least one day before measurements and are manipulated with gloves. For convenience, when transfer impedance and input impedance are both required quantities are measured over the whole frequency range successively (not simultaneously).

5.2. CALIBRATION RESULTS FOR INPUT IMPEDANCE

Since the procedure is inaccurate for low frequencies, the low-frequency response of the sensor which can be modelled as a first order low-pass cut-off frequency, cannot be accurately determined using the proposed procedure. This cut off is then determined using the short tube as a cavity: the cut-off frequency can be deduced from the phase shift. For the present sensor it is found to be approximately 15 Hz.

The approximation K of the first order response for higher frequencies is determined using the procedure described in Part I; i.e., from the input impedance of a long tube the mean line of a dB plot of the amplitude gives the amplitude response ($|K|$) and the mean line of the phase gives the phase response ($Arg(K)$). The complex response is related to the response of the microphone cartridge as shown in reference [15].

Since low-frequency response has been determined separately, the calibration parameters were fitted with a polynomial function with positive exponent which is little influenced by low-frequency variations. It appears that for frequencies lower than 4 kHz the amplitude response (in dB, which corresponds to real part of $g \ln KZ_c$), is parabolic without a linear term (second order filter due to the spring–mass effect of the membrane), the phase response (imaginary part of $g \ln KZ_c$) is linear (i.e., a pure delay) together with corrective effects due to higher modes (i.e., a subtracted mass effect) and impedance of the source (equivalent volume). Real parts of b and d are reasonably well approximated by a square root of frequency. This leads to only nine calibration parameters. For higher frequencies (typically beyond 4 kHz, the high cut-off frequency of the tube being approximately 10 kHz for a 20 mm diameter tube) this is no longer valid mainly because the first higher mode effect becomes more important and can no longer be approximated as a subtracted mass effect at the input of the tube. Higher modes affect not only parameters b and d but also the response g. However, the total number of parameters for the three complex calibration functions do not exceed 25 for a calibration from 0 to 8 kHz.

Reproducibility is good when measurements are made the same day but less so when measurements are repeated after a few days. For accurate measurements, a calibration must be done for every series of measurements. Since this takes less than 30 min this is not a problem.

After calibration, the validity of the measurements can be verified. The measured impedance, i.e., the measured input pressure computed with the calibration function, of a closed tube can be compared with the theoretical expression of the input impedance of the tube. In fact, the quantity obtained initially is the reduced impedance $z_r = Z/Z_c$. As this is theoretically given by equation (B2) the propagation constant can be deduced (Figure 5) and compared to its theoretical expression (see Appendix B) plotted in Figure 2. The comparison with the real part of Γ shows that the difference between the theoretical and experimental values is approximately 3% for $f < 5$ kHz (see Figure 6). As the theoretical value of α is not known with an accuracy better than 2% these results can be considered as acceptable. This result shows that the theoretical expression of Γ can be used in computation of pressure measurements in tubes when the metal tubes are not too large and sufficiently stiff.

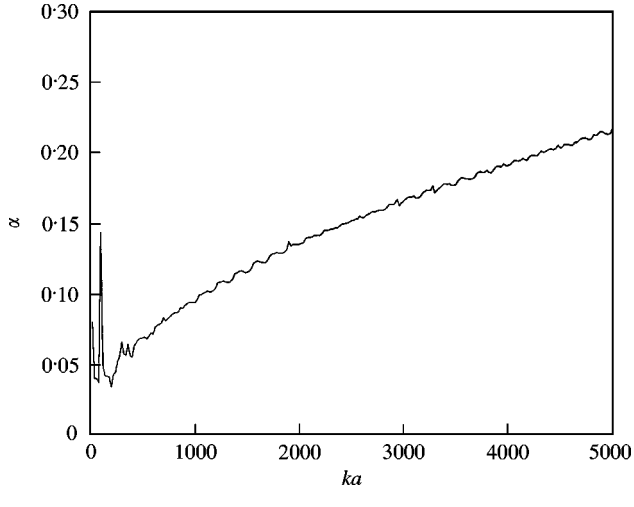

Figure 5. Experimental value of the attenuation constant α for a closed 1 m tube of radius 0·01 m versus reduced frequency ka after a complete calibration.

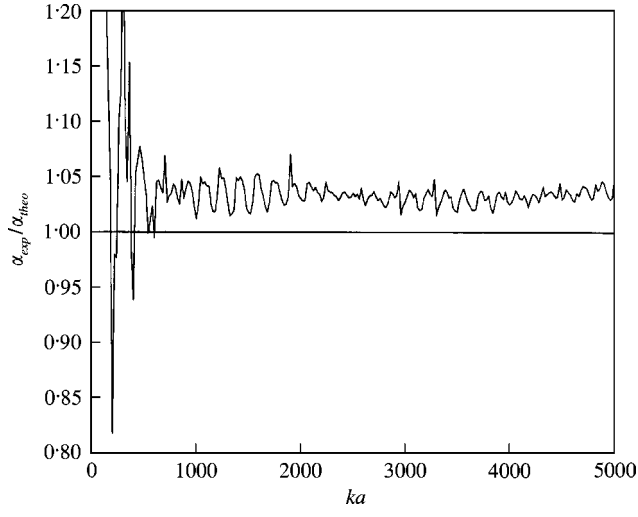

Figure 6. Ratio of experimental and theoretical value of the attenuation constant α of a 1 m tube of radius 0·01 m.

5.3. CALIBRATION RESULTS FOR TRANSFER IMPEDANCE

In the description of the method applied to symmetrical two-port elements, it is assumed that the termination impedance with a microphone is infinite. If not, this impedance has to be determined. This can be deduced from the input impedance measurement of a short tube with this termination where the calibration is made with the same tube terminated with a rigid cap without a microphone. It appears that there is no significant difference between the two measurements other than a possible 0·1 mm length difference which can be ascribed to differences in the geometry of the caps.

The function K was taken to be identical for both input and transfer impedances, but response g_2 appears to be different from response g_1. This may be explained by the difference in sensitivity of the two receiver microphones (approximately 6 dB). The frequency dependence of these two parameters is also slightly different. The evaluation of the parameter d_1 is very close (as it should) to the one obtained from the input impedance.

The transfer impedance as well as the input impedance can be compared to theory and the propagation constant can be deduced. Results are very similar to those deduced from the input impedance but are much more noisy (Figure 7). This can be explained by the fact that when Z_{12} is close to unity an error ε on Z_{12} implies an error of $\sqrt{2\varepsilon}$ on $\arg \cosh(Z_c/Z_{12}) = \Gamma L$ which is much larger than ε. Despite this, results can be considered as satisfactory and measurements of Z_{12} can be considered to be quite accurate.

6. APPLICATION TO THE MEASUREMENT OF AN OPEN SIDE HOLE

The theory of a branched tube, initiated by Keefe [17, 18] has recently achieved a high degree of accuracy [19, 20]. This accuracy is needed especially for the modelling of woodwind instruments whose resonance frequencies are dependent on the side hole characteristics. A short-branched tube can be considered as a two port and characterized by its transfer matrix $\left(\begin{smallmatrix} A & B \\ C & D \end{smallmatrix}\right)$ or an equivalent electrical circuit (see Figures 8 and 9). This transfer matrix cannot be determined directly because the side hole cannot be considered alone but has to be incorporated in a piece of tube. For the measurements the side hole was positioned in the middle of a closed tube of length $2L$. The system being symmetrical the

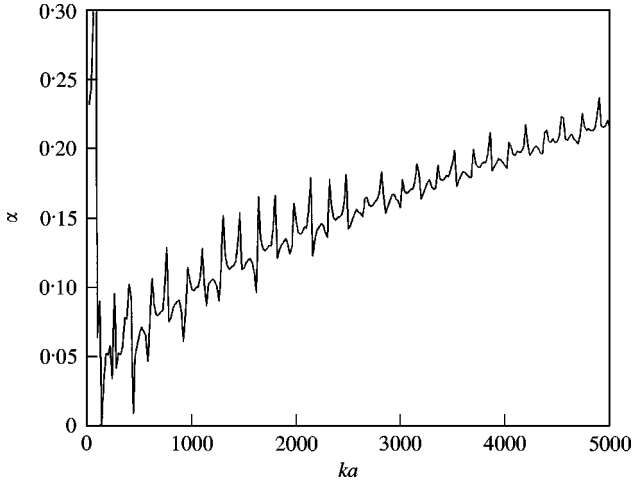

Figure 7. Experimental value of $\alpha = \text{Re}[\arg\sinh(Z_c/Z_t)]/\ell$ for a closed 1 m tube of radius 0·01 m versus reduced frequency ka after a complete calibration.

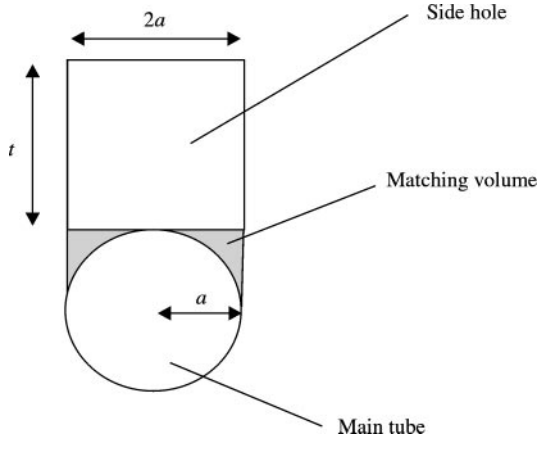

Figure 8. Dimensions definition for a side hole in a cylindrical tube.

measurement of the input impedance Z_{11} and of the transfer impedance Z_{12} is sufficient to determine the transfer matrix of the system (see equation (A1) in Appendix A). The transfer matrix of the side hole itself is then obtained by multiplying, left and right, the transfer matrix of the system by the inverse matrix of a tube of length L. Measurements have been carried out with the sensor described above for a side hole of radius $a = 10$ mm and height $t = 10{\cdot}25$ mm on a closed tube of same diameter and length $2L = 100$ mm (see Figure 8). The side hole was terminated with a "normalized" flange because the corresponding impedance is in that case accurately known (see reference [21] for description and discussion). Results for the imaginary part of 1/C and B are given in Figure 10. Results can be compared with theoretical results. As $1/C = Z_i + Z_o$, according to Nederveen *et al.* [19] and Dubos *et al.* [20] $Z_i = \text{j}Z_c kt_i$ and $Z_o = \text{j}Z_c \tan[k(t + t_m + \delta)]$ where $t = 1{\cdot}025a$ is the height of the cylindrical part of the branched tube, $t_m = 0{\cdot}15a$ is the ratio of the matching volume between the main tube and the branched tube to the cross-section of the branched tube (see Figure 8 and references [19, 20] for the calculation of this volume), δ is the

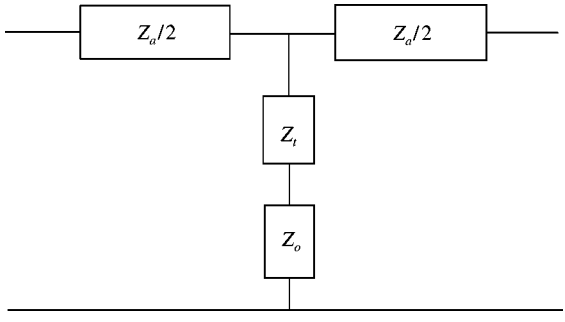

Figure 9. Equivalent electrical circuit for the side hole.

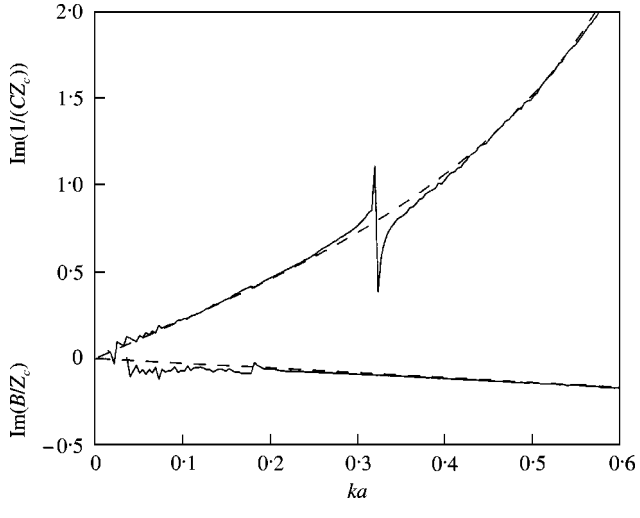

Figure 10. Imaginary parts of terms B (lower) and 1/C (upper) of the transfer matrix of an open side hole of 10·5 mm long and radius 10 mm ended with a normalized flange on a tube of radius 10 mm versus reduced frequency ka: ———, experiment; - - - - - - - -, theory.

radiation length correction and is given in reference [21] to be for the normalized flange:

$$\delta = 0{\cdot}81a\left[1 + \frac{(0{\cdot}77\,ka)^2}{1 + 0{\cdot}77ka}\right]^{-1}$$

and t_i is the inner length correction which is given to be $t_i = 0{\cdot}17a$ by both references [19, 20] $B = Z_a[1 + Z_a/4(Z_t + Z_0)] \approx Z_a$ where $Z_a/Z_c = \mathrm{j}kt_a$ with t_a given to be $t_a = -0.28a$ by both references [19, 20]. Experimental results are in a good agreement with theory for the present hole diameter. It must be noted that results for C are not accurate when $\sin(kL) \approx 0$. In that case, the side hole shunt impedance does not come into play because of the pressure antinode in the middle of the tube. For these frequencies another measurement configuration would be needed. This is a subject for further experiments.

7. CONCLUSIONS

The proposed calibration method is a powerful tool for improving the accuracy of acoustic impedance sensors by optimizing their calibration. It determines second order

effects which are often neglected. However, the number of constants to be determined in this calibration method leads to a reduced number of parameters. Moreover, the calibration method is shown to be valid for most of impedance sensors. A major advantage is that the wave constant of the calibration tubes does not need to be known exactly, making the measurements less sensitive to temperature measurement errors. Apart from that the method allows the determination of the propagation constant of which the real part is, for a standard plumbing tube, shown to be less than 3% higher than predicted by theory. This method has been applied to a sensor using a half-inch microphone cartridge as a source of volume velocity and this calibrated set-up has been used already for input impedance measurements of wind instruments [22, 23]. In a companion paper, it is used as well for radiation impedance measurements [21]. The extension to impedance matrix measurements has been successfully realized, giving the opportunity to measure the characteristics of multi-port systems. For example, the method is applied to side hole measurements and is shown to be sufficiently accurate to deduce the characteristics of such lumped elements.

ACKNOWLEDGMENTS

Others who have worked with the author over the past 10 years, on the problem of impedance set-up calibration include Anne-Marie Bruneau and Jean Kergomard who initiated this study, Philippe Herzog with whom the author has held fruitful discussions, and Sylvain Poggi and Simon Félix who worked on the algorithm. Finally, the author would like to thank Kees Nederveen and Murray Campbell for reviewing this paper.

REFERENCES

1. H. Bodén and M. Åbom 1986 *Journal of the Acoustical Society of America* **79**, 541–549. Influence of errors on the two-microphone method for measuring acoustic properties in ducts.
2. H. Bodén and M. Åbom 1988 *Journal of the Acoustical Society of America* **83**, 2429–2438. Errors analysis of two-microphone measurements in ducts with flow.
3. V. Gibiat and F. Laloë 1990 *Journal of the Acoustical Society of America* **88**, 2533–2545. Acoustical impedance measurements by the two-microphone-three-calibration (TMTC) method.
4. D. H. Keefe 1996 *Journal of the Acoustical Society of America* **99**, 2370–2381. Wind instrument reflection function measurements in the time domain.
5. J. P. Dalmont and Ph. Herzog 1993 *Acoustics* '93, *Southampton*, *Proceedings of the Institute of Acoustics*, Vol. **15**, 681–688. Improved analysis of input impedance measurements.
6. A. H. Benade and M. I. Ibisi 1987 *Journal of the Acoustical Society of America* **81**, 1152–1167. Survey of impedance methods and a new piezo-disk-driven impedance head for air columns.
7. A. M. Bruneau 1987 *Journal of the Acoustical Society of America* **81**, 1168–1178. An acoustic impedance sensor with two reciprocal transducers.
8. J.-P. Dalmont 2001 *Journal of Sound and Vibration* **243**, 427–439. Acoustic impedance measurement, Part I: a review.
9. R. Causse, J. Kergomard and X. Lurton 1984 *Journal of the Acoustical Society of America* **75**, 241–254. Input impedance of brass instruments—comparison between experiment and numerical models.
10. A. F. Seybert and D. F. Ross 1977 *Journal of the Acoustical Society of America* **61**, 1362–1370. Experimental determination of acoustic properties using a two-microphone random-excitation technique.
11. J. Y. Chung and D. A. Blaser 1980 *Journal of the Acoustical Society of America* **68**, 907–913. Transfer function method of measuring in-duct acoustic properties. I Theory.
12. J. Y. Chung and D. A. Blaser 1980 *Journal of the Acoustical Society of America* **68**, 914–921. Transfer function method of measuring in-duct acoustic properties. II Experiment.
13. J. Y. Chung and D. A. Blaser 1980 *Journal of the Acoustical Society of America* **68**, 1570–1577. Transfer function method of measuring acoustic intensity in a duct system with flow.

14. W. T. CHU 1986 *Journal of the Acoustical Society of America* **80**, 347–348. Extension of the two-microphone transfer function method for impedance tube measurements.
15. J. P. DALMONT and A. M. BRUNEAU 1992 *Journal of the Acoustical Society of America* **91**, 3026–3033. Acoustic impedance measurements: plane-wave mode and first helical mode contributions.
16. M. BRUNEAU 1983 *Introduction aux théories de l'acoustique*. Université du Maine Editeur.
17. D. H. KEEFE 1982 *Journal of the Acoustical Society of America* **72**, 676–687. Theory of the single woodwind tone hole.
18. D. H. KEEFE 1982 *Journal of the Acoustical Society of America* **72**, 688–699. Experiments on the single woodwind tone hole.
19. C. J. NEDERVEEN, J. K. M. JANSEN and R. R. van HASSEL 1998 *ACUSTICA united with Acta Acustica* **84**, 957–966. Corrections for woodwind tone-hole calculations.
20. DUBOS, J. KERGOMARD, D. KEEFE, J.-P. DALMONT, A. KHETTABI and K. NEDERVEEN 1999 *ACUSTICA united with Acta Acustica* **85**, 153–169. Theory of sound propagation in a duct with a branched tube using modal decomposition.
21. J.-P. DALMONT, K. NEDERVEEN and N. JOLY 2000 *Journal of Sound and Vibration*. Radiation Impedance of tube ended with different flanges: numerical and experimental investigations. (Submitted).
22. B. GAZENGEL, J. GILBERT and N. AMIR 1995 *Acta Acustica* **3**, 445–472. Time domain simulation of single reed wind instrument. From the measured input impedance to the synthesis signal. Where are the traps.
23. J.-P. DALMONT and J. KERGOMARD 1994 *Acta Acoustica* **2**, 223–232. Lattices of sound tubes with harmonically related eigenfrequencies.
24. A. D. PIERCE 1981 *Acoustics*. New York: McGraw-Hill.
25. D. H. KEEFE 1984 *Journal of the Acoustical Society of America* **75**, 58–62. Acoustical wave propagation in cylindrical ducts: transmission line parameter approximations for isothermal and non isothermal boundary conditions.
26. M. BRUNEAU 1998 *Manuel d'acoustique fondamentale*. Paris: HERMES.

APPENDIX A: RELATION BETWEEN IMPEDANCE AND TRANSFER MATRICES FOR A TWO-PORT

The impedance matrix relates the pressure vector to the volume velocity vector for a two port:

$$\begin{pmatrix} P_1 \\ P_2 \end{pmatrix} = \begin{pmatrix} Z_{11} & Z_{12} \\ Z_{21} & Z_{22} \end{pmatrix} \begin{pmatrix} U_1 \\ U_2 \end{pmatrix}. \tag{A1}$$

Note that the volume velocity is considered positive when entering the system (symmetrical orientation).

The transfer matrix for a two port relates pressure and volume velocity on port 1 (the input) to pressure and volume velocity on port 2:

$$\begin{pmatrix} P_1 \\ U_1 \end{pmatrix} = \begin{pmatrix} A & -B \\ C & -D \end{pmatrix} \begin{pmatrix} P_2 \\ U_2 \end{pmatrix} \tag{A2}$$

for a symmetrical orientation. It is often convenient to consider both the volume velocity going into the input and the volume velocity going out from the output (antisymmetrical orientation) to be positive. In that case, the transfer matrix is $\left(\begin{smallmatrix} A & B \\ C & D \end{smallmatrix}\right)$.

It is easy to derive

$$\begin{pmatrix} A & B \\ C & D \end{pmatrix} = \begin{pmatrix} Z_{11}/Z_{21} & (Z_{11}Z_{22} - Z_{12}Z_{21}/Z_{12}) \\ 1/Z_{21} & Z_{22}/Z_{21} \end{pmatrix}. \tag{A3}$$

For a reciprocal system: $Z_{12} = Z_{21} \Leftrightarrow AD - BC = 1$ and for a symmetrical system, $Z_{11} = Z_{22} \Leftrightarrow A = D$.

APPENDIX B: CHARACTERISTICS OF A STRAIGHT TUBE

For a straight tube of length L the transfer matrix is given by

$$\begin{pmatrix} A & B \\ C & D \end{pmatrix} = \begin{pmatrix} \cosh \Gamma L & Z_c \sinh \Gamma L \\ \dfrac{\sinh \Gamma L}{Z_c} & \cosh \Gamma L \end{pmatrix}, \tag{B1}$$

where Z_c is the characteristic impedance and Γ the propagation constant. Γ is given, for a circular tube with rigid wall, by

$$\Gamma = \mathrm{j}k + (1 + j)\alpha,$$

where $k = \omega/c = 2\pi f/c$ is the wave number. α is the attenuation constant and is given accurately by

$$\alpha = \frac{1}{a}\sqrt{\frac{\omega}{2c}}\,(\sqrt{\ell_v} + (\gamma - 1)\sqrt{\ell_h})$$

with a radius of the tube (see for example references [24–26]).

This formula is valid for $a\sqrt{\omega/c\ell_h} \gg 1$. In the air in standard condition is [9]

$$c = 331.45\sqrt{1 + \frac{t}{T_0}}\ \mathrm{m/s\ with}\ T_0 = 273{\cdot}15\,\mathrm{K},$$

$$\ell_v = 3{\cdot}986 \times 10^{-8}(1 + 4{\cdot}73 \times 10^{-3}t)\,\mathrm{m},$$

$$\ell_h = 5{\cdot}61 \times 10^{-8}(1 + 5{\cdot}13 \times 10^{-3}t)\,\mathrm{m},$$

$$\gamma = 1{\cdot}4024(1 - 2{\cdot}1 \times 10^{-5}t)\,\mathrm{m}.$$

At 20°C this leads to $\alpha = 2{\cdot}96 \times 10^{-5}\sqrt{f}/a$ with f in Hz and a in metres. Z_c is given by

$$Z_c = \frac{\rho c}{S}(1 + (1 - j)\beta/k)$$

with $\beta = 1/a\sqrt{\omega/2c}\,(\sqrt{\ell_v} - (\gamma - 1)\sqrt{\ell_h})$.
At 20°C this leads to $\beta = 0{\cdot}82 \times 10^{-5}\sqrt{f/a}$ with f in Hz.

At 100 Hz, for a 10 mm diameter tube, $\beta/k = 0{\cdot}004$ and is most often neglected. Note that with the same data $a\sqrt{\omega/c\ell_h} \approx 100$ which is sufficient to consider the previous formulae as accurate with an error lower than 1% for frequencies larger than 200 Hz.

When there is no source on port 2, it can be assumed that $U_2/P_2 = Y_t$ where Y_t is the admittance at the end of the tube. The input impedance is then given by

$$Z = \frac{P_1}{U_1} = Z_c\frac{\cosh(\Gamma L) + Z_c Y_t \sinh(\Gamma L)}{\sinh(\Gamma L) + Z_c Y_t \cosh(\Gamma L)} = Z_c \coth\left[\Gamma L + \operatorname{arctanh}(Z_c Y_t)\right]. \tag{B2}$$

The impedance matrix is given by

$$Z_{11} = Z_{22} = Z_c \coth[\Gamma L] \quad \text{and} \quad Z_{12} = Z_{21} = Z_c / \sinh[\Gamma L].$$

It can be verified that, when $Y_t = 0$, $Z = P_1/U_1 = Z_{11}$ and $Z_{tr} = P_2/U_1 = Z_{21}$.

APPENDIX C: PROOF OF EQUATION (13)

It is shown here how equation (13) is derived from equations (11 and 12)

(1) Write $z_r'' = (z_r' + \tanh d)/(1 - z_r' \tanh d)$ and attempt to find an expression for $\Gamma L'' = \text{arctanh}\,(1/z_r'')$.

Expressing $z_r' = \coth(\Gamma L')$ and $\tanh d$ with exponential functions it can be shown that

$$z_r'' = \frac{e^{+(\Gamma L' + d)} + e^{-(\Gamma L' + d)}}{e^{+(\Gamma L' - d)} - e^{-(\Gamma L' - d)}}.$$

$\Gamma L''$ is then given by

$$\Gamma L'' = \text{arctanh}(1/z_r'') = \frac{1}{2}\ln\left(\frac{z_r'' + 1}{z_r'' - 1}\right) = \Gamma L' + \frac{1}{2}\ln\left(\frac{1 - e^{-2\Gamma L'} \tanh d}{1 + e^{+2\Gamma L'} \tanh d}\right).$$

Assuming $d \ll 1$ a first order development leads to

$$\Gamma L'' \approx \Gamma L' - d \cosh(2\Gamma L').$$

(2) Write $H/KZ_c = z_r''' = e^g z_r''$ and attempt to find an expression for $\Gamma L''' = \text{arctanh}\,(1/z_r''')$.

Expressing $z_r'' = \coth(\Gamma L'')$ with exponential functions it can be shown that

$$z_r''' = \frac{e^{+(\Gamma L'' + g)} + e^{-(\Gamma L'' - g)}}{e^{+(\Gamma L'')} - e^{-(\Gamma L'')}}.$$

$\Gamma L'''$ is then given by

$$\Gamma L''' = \frac{1}{2}\ln\left(\frac{z_r''' + 1}{z_r''' - 1}\right) = \Gamma L'' + \frac{1}{2}\ln\left(\frac{1 + e^{-2\Gamma L'} \tanh(g/2)}{1 + e^{+2\Gamma L'} \tanh(g/2)}\right).$$

Assuming $g \ll 1$ a first order development leads to

$$\Gamma L''' \approx \Gamma L'' - \frac{g}{2}\sinh(2\Gamma L'').$$

(3) Finally,

$$\Gamma L''' \approx \Gamma L' - d \cosh(2\Gamma L') - \frac{g}{2}\sinh(2\Gamma L'').$$

For simplicity, in the previous expression, $\Gamma L''$ can be assumed to be equal to $\Gamma L'$. By writing $\Gamma L' = \mathrm{j}kL' + \alpha L'$:

$$\mathrm{Re}\left(\operatorname{arctanh}\left(\frac{H}{KZ_c}\right)\right) \cong \alpha L' - \left[\mathrm{Re}\left(\frac{g}{2}\right)\sinh(2\alpha L') + \mathrm{Re}(d)\cosh(2\alpha L')\right]\cos(2kL') + \left[\mathrm{Im}\left(\frac{g}{2}\right)\cosh(2\alpha L') + \mathrm{Im}(d)\sinh(2\alpha L')\right]\sin(2kL') \tag{C1a}$$

and

$$\mathrm{Im}\left(\operatorname{arctanh}\left(\frac{H}{KZ_c}\right)\right) \cong kL' - \left[\mathrm{Im}\left(\frac{g}{2}\right)\sinh(2\alpha L') + \mathrm{Im}(d)\cosh(2\alpha L')\right]\cos(2kL') - \left[\mathrm{Re}\left(\frac{g}{2}\right)\cosh(2\alpha L') + \mathrm{Re}(d)\sinh(2\alpha L')\right]\sin(2kL'). \tag{C1b}$$